Advanced Steel Construction – Vol. 18 No. 2 (2022) 574–584
DOI:10.18057/IJASC.2022.18.2.6

THEORETICAL STUDY ON EARLY STAGE SELF-LOOSENING OF BOLTED JOINT IN LATTICE TRANSMISSION TOWER UNDER TRANSVERSE LOAD

Wen-Qiang Jiang [1 *], Ze Mo [1], Lan-Qi Yang [1], Jing-Li Liu [2], Zhuo-Bo Niu [2] and Li-Qiang An [1,3]

[1] *Department of Mechanical Engineering, North China Electric Power University, BaoDing, P. R. China*
[2] *Baoding Power Supply Company, Baoding, P. R. China*
[3] *Hebei Key Laboratory of Electric Machinery Health Maintenance & Failure Prevention, North China Electric Power University, BaoDing, P. R. China*
** (Corresponding author: E-mail: wenqiang.jiang@ncepu.edu.cn)*

ABSTRACT

Bolted joints are one of the key components of lattice transmission towers. Under alternating transverse loads, the preload of bolted joints will be reduced, which may cause bolt loosening and consequently change the inherent mechanical properties of the bolted joints and eventually trigger the structure failure. In order to study the critical loosening load of bolted joint in lattice transmission tower under the transverse load, the mechanical models of bolted joint with single shear plane and double shear planes are established. A new theoretical method of critical loosening load with considering the deformation of bolt screw threads is derived. The thread stresses of two typical bolted joints are given and compared with that from finite element method, which verified the accuracy of the new analytical method. The influences of bolt preload, friction coefficient of thread surface, bolt clamping length and number of shear planes on the critical loosening load of bolts are studied.

ARTICLE HISTORY

Received: 18 March 2021
Revised: 25 September 2021
Accepted: 10 October 2021

KEYWORDS

Lattice transmission tower;
Bolted joint;
Bolt loosening;
Transverse load;
Theoretical study

1. Introduction

Lattice towers are widely used all over the world as supporting structures in power grids, which are commonly constructed of angle section (L-shape) members connected by bolted joints[1]. Typical bolted joints in lattice tower are single leg bolted joint in diagonal member and lap splice bolted joint in leg member (as shown in Fig. 1), which has one shear plane and two shear planes respectively[2]. In practice, the lattice transmission tower often suffering from dynamic loads, such as wind loads, ice shedding, conductor galloping and etc[3]. Therefore, bolted joints in lattice transmission tower are usually worked under dynamic loads, which may cause the self-loosening of bolts and lead to the decline of clamping force. The changing of bolt clamping force may lead to the change of inherent characteristic of bolted joint and the whole structure, result in the failure of members or cascading failure of lattice tower[4-6]. Fig. 2 shows the tower cross-arm failure accident in 500kV Fengzhang line of the State Grid Corporation of China due to the conductor galloping in the early spring of 2014. Due to conductor galloping, alternate forces are loaded on the tower structure and bolted joints, which led to the bolt self-loosening and even falling down from the tower. Therefore, the tower cross-arms are weakened and has a tendency to form fatigue damage. The above presented failure modes of transmission tower caused by self-loosening of bolt happen occasionally, and it is difficult to detect in regular inspection as the number of bolted joints is numerous, which is a serious threat for the operation of power lines. Therefore, it is necessary to study the critical loosening load of the bolted joint to avoid the joint failure in lattice tower.

In order to insure the safety of lattice tower, lots of researchers focus on the mechanical behavior prediction of lattice tower. In the numerical approaches, the geometric nonlinearity, material nonlinearity, second-order effects and joint effects are included to improve the accuracy[7-9]. Many researchers pointed out that the joint stiffness affects the mechanical behaviour of lattice tower greatly. Therefore, lots of joint models are presented and introduced in the numerical models of lattice tower[10]. However, in those numerical approaches, the looseness of the bolted joint has not been included, which may cause error in the analysis of the transmission tower structure by the direct nonlinear analysis method.

In the direct nonlinear analysis of structures, the joint model with considering bolt preload status can lead to more precise results[11]. However, the critical self-loosening load of bolted joint should be determined before the bolt preload statuses are obtained. In the early stage of bolted joint self-loosening, the local slip of the thread surface will gradually accumulate under the action of the transverse cyclic load[12]. When the local slip on the thread surface accumulates to a certain degree, the torque of the thread surface will decrease, the thread contact surface is prone to overall slip, and the nut and the bolt will rotate relative to each other. The bolted joint will failure when the rotation of the bolt and nut reaches a certain degree. Therefore, the local slip of the thread surface will directly cause bolt loosening[13]. From the perspective of the deformation of the bolt, the bending deformation of the bolt shank will led to the periodically change of contact stress on thread surface under transverse load[14]. Meanwhile, the deformation of the threads will make the local friction of the thread contact surface easily overcome, resulting in local slip of the thread surface[15]. Obviously, the deformation of bolt shank and thread has important effects on the early stage bolted joint self-loosening.

In this paper, the typical bolted joints in lattice transmission tower with one or two shear planes are studied. The calculation method of thread stress is verified by finite element model, and a new theoretical calculation method is presented to determine the critical load of early bolt self-loosening. The influence of the bolt joint parameters is discussed in detail to illustrate how to prevent the self-loosening of the bolts in the transmission tower.

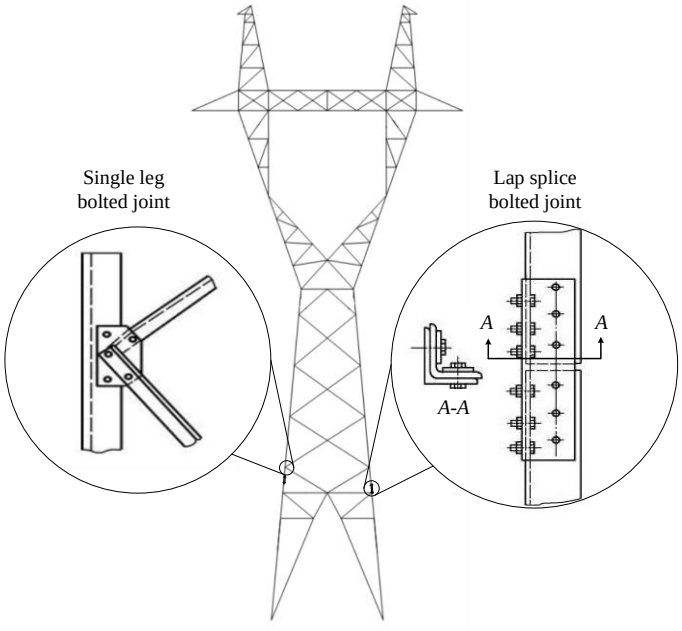

Fig. 1 Bolted joint in lattice transmission tower

Fig. 2 Tower cross-arm failure accident caused by bolts loosening

2. Mechanical model of bolted joint

In traditional lattice transmission tower, the axis of tower members is perpendicular to the bolts axis in connection. Therefore, the bolted joint will work under transverse load, as shown in Fig. 3 and Fig. 4.

As can be seen in Fig. 3a, for the single leg bolted joint in diagonal member, there is only one shear plane. For the single shear plane bolted joint under transverse load, the friction between nut and the gusset will lead to the bending of bolt shank. However, the macroscopic slippage of bolt shank and nut will not occur until the self-loosening critical load of bolt reached[14]. Therefore, the bolt head and nut are still stick on the gusset surface, and their rotations are restricted. Fig. 3b shows the mechanical model of single shear plane bolted joint, and it can be equivalent substitution by Fig. 3c.

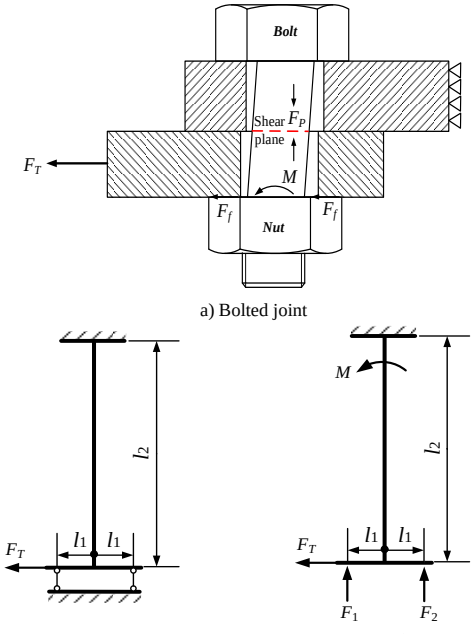

a) Bolted joint

b) Mechanical Model c) FBD of Bolt

Fig. 3 Single shear plane bolted joint under transverse load

The problem shows in Fig. 3c can be easily solved by linear superposition method. Since the clamping length l_2 of the bolt is much larger than the clearance l_1 between the bolt shank and the bolt hole, the influence of the clearance l_1 on the bending moment of the bolt is ignored. The friction F_f and the additional bending moment M can be get separately

$$F_f = F_T \qquad M = \frac{1}{2}F_T l_2 \tag{1}$$

However, for the lap splice bolted joint in tower main leg member, there are two shear planes as shown in Fig. 4. For the bolted joint with double shear planes, there will be no obvious load on the bolt before the clearance of middle gusset hole disappeared, as the top and bottom gusset are deformed simultaneously. However, after the slippage stopping, the contact between bolt shank and hole will produce friction between nut and gusset. Based on the same assumptions as single shear plane bolted joint, the bolt head and the nut are considered to stick on the gusset surfaces and their rotations are restricted before self-loosening occurring. Fig. 4b shows the mechanical model of double shear planes bolted joint, and it can be equivalent substitution by Fig. 4c.

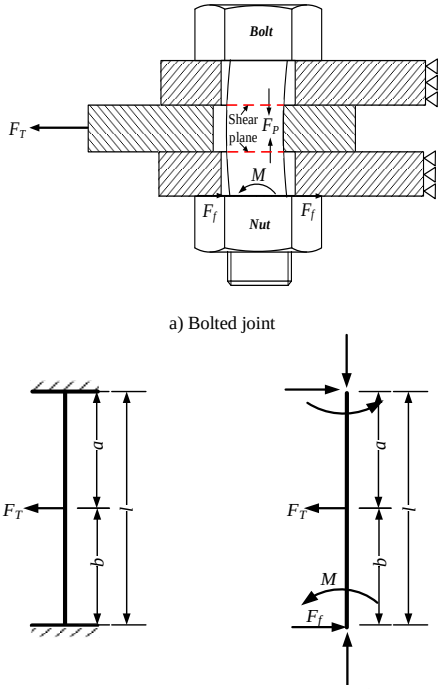

a) Bolted joint

b) Mechanical Model c) FBD of Bolt

Fig. 4 Double shear planes bolted joint under transverse load

The problem shows in Fig. 4c also can be solved by linear superposition method. The friction F_f and the additional bending moment M can be get separately

$$F_f = \frac{F_T a^2}{l^2}\left(1+\frac{2b}{l}\right) \tag{2}$$

$$M = -\frac{F_T a^2}{l^2}(l-a) \tag{3}$$

When $a = l/2$, the equation (2) and (3) are simplified as

$$F_f = \frac{F_T}{2} \qquad M = -\frac{1}{8}F_T l \tag{4}$$

As can be seen in equation (1) and (4), it is obviously that the friction between the gussets and nut and additional bending moment will be effected by the number of shear planes. For the same transverse load F_T, the friction of double shear planes bolted joint is half of single shear plane bolted joint, and the additional bending moment is only a quarter of single shear plane bolted joint acting on the opposite direction.

3. Critical conditions of bolt self-loosening

In practice, there are many types of thread, such as rectangle thread, triangle thread, trapezoid thread and etc. In lattice transmission tower bolted joint, the triangle thread is commonly used. Therefore, the critical conditions of bolt self-loosening with triangle thread are presented, which can be easily used in other threads.

3.1. Mechanical analysis of thread

The forces act on the thread are preload F_p, additional bending moment M and the friction force F_f （See Fig. 3a and Fig. 4a） when the bolted joint worked under transverse load, which should be included in the analysis of thread. In order to study the critical conditions of bolt self-loosening, the detail geometry of thread should be considered. The global Cartesian coordinate system with ordinate origin O located at the intersection point of bolt axis and bearing surface of nut is established, as shown in Fig. 5.

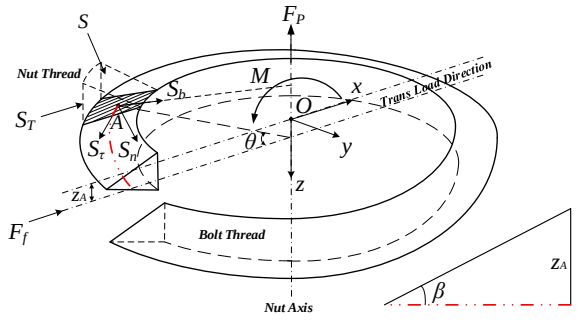

Fig. 5 FBD of bolt thread

In Fig. 5, θ is the angle between the radial direction of the bolt shank cross-section at point *A* and the transverse load direction. z_A is the corresponding height of point *A* in the direction of z-axis. Expand the thread from the initial point to the current position. The two-dot chain line in Fig. 5 is the projection of the unfolded thread on the cross section of the bolt at z_A. Therefore, for any point on the thread , the relationship between height *z* and angle θ can be expressed as

$$z = \frac{d_2}{2} \cdot \theta \cdot tg\beta \tag{5}$$

Where, d_2 is the thread diameter and β is the helix angle of thread.

It has been proved that the local slippage of the thread is an important reason of bolt loosening[11-12]. Therefore, it is necessary to analyze the force on the micro area of the thread surface. As shown in Fig.5, a local natural coordinate is established, and the forces on the micro area of unit length around point *A* on the nut thread are presented. Since the radial dimension of the thread is small compared with the diameter of the bolt or nut, it is assumed that the force on the thread face is even in the radial direction of the thread. S_τ, S_n and S_b represent the component forces of tangential, normal and radial forces loaded on this micro-region. S_T is the transverse load on the nut thread caused by the F_f, and S is the resultant forces due to the bolt preload F_p and the additional bending moment M.

In order to simplify the derivation, the relationship between global Cartesian coordinate (x, y, z) and local natural coordinate (b, τ, n) on the thread should be presented firstly. As shown in Fig. 6, the local natural coordinate can be got by rotating the global Cartesian coordinate around its axis by the following three steps: a) Rotate θ about z-axis; b) Rotate $-\beta$ about x-axis; c) Rotate α about y-axis, in which α is the thread angle.

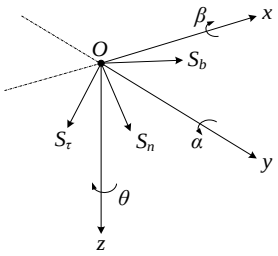

Fig. 6 Relationship between global Cartesian coordinate and local natural coordinate

According to the coordinate transformation rules, the relationship of global Cartesian coordinate (x, y, z) and local natural coordinate (b, τ, n) can be given as below.

$$\begin{bmatrix} x \\ y \\ z \end{bmatrix} = \boldsymbol{T} \cdot \begin{bmatrix} b \\ \tau \\ n \end{bmatrix} \tag{6}$$

in which,

$$\boldsymbol{T} = \boldsymbol{T}_1 \cdot \boldsymbol{T}_2 \cdot \boldsymbol{T}_3$$

$$\boldsymbol{T}_1 = \begin{bmatrix} \cos\theta & -\sin\theta & 0 \\ \sin\theta & \cos\theta & 0 \\ 0 & 0 & 1 \end{bmatrix} \quad \boldsymbol{T}_2 = \begin{bmatrix} 1 & 0 & 0 \\ 0 & \cos\beta & \sin\beta \\ 0 & -\sin\beta & \cos\beta \end{bmatrix} \quad \boldsymbol{T}_3 = \begin{bmatrix} \cos\alpha & 0 & \sin\alpha \\ 0 & 1 & 0 \\ -\sin\alpha & 0 & \cos\alpha \end{bmatrix}$$

The transform matrix can be easily calculated by multiplied matrix $\boldsymbol{T}_1$, $\boldsymbol{T}_2$ and $\boldsymbol{T}_3$.

$$\boldsymbol{T} = \begin{bmatrix} \cos\theta\cos\alpha + \sin\theta\sin\beta\sin\alpha & -\sin\theta\cos\beta & \cos\theta\sin\alpha - \sin\theta\sin\beta\cos\alpha \\ \sin\theta\cos\alpha - \sin\alpha\cos\theta\sin\beta & \cos\theta\cos\beta & \sin\theta\sin\alpha + \cos\theta\sin\beta\cos\alpha \\ -\sin\alpha\cos\beta & -\sin\beta & \cos\beta\cos\alpha \end{bmatrix} \tag{7}$$

Based on the force balance condition on the micro-region *A*, the balance equations can be derived as following

$$\begin{aligned} &S_b(\cos\theta\cos\alpha + \sin\theta\sin\beta\sin\alpha) - (S_\tau - S\sin\beta)\sin\theta\cos\beta \\ &+(S_n + S\cos\beta)(\cos\theta\sin\alpha - \sin\theta\sin\beta\cos\alpha) + S_T = 0 \end{aligned} \tag{8}$$

$$\begin{aligned} &S_b(\sin\theta\cos\alpha - \sin\alpha\cos\theta\sin\beta) + (S_\tau - S\sin\beta)\cos\theta\cos\beta \\ &+(S_n + S\cos\beta)(\sin\theta\sin\alpha + \cos\theta\sin\beta\cos\alpha) = 0 \end{aligned} \tag{9}$$

$$-S_b\sin\alpha\cos\beta - (S_\tau - S\sin\beta)\sin\beta + (S_n + S\cos\beta)\cos\beta\cos\alpha = 0 \tag{10}$$

Therefore, S_τ, S_b and S_n can be calculated by combining the equation (8), (9) and (10).

$$S_\tau = S_T\sin\theta\cos\beta + S\sin\beta \tag{11}$$

$$S_n = S_T(\sin\theta\sin\beta\cos\alpha - \cos\theta\sin\alpha) - S\cos\beta \tag{12}$$

$$S_b = -S_T(\cos\theta\cos\alpha + \sin\beta\sin\theta\sin\alpha) \tag{13}$$

The condition that the micro area of the thread contact surface does not produce relative slip is that the total force of the external load along the tangential direction of the thread surface is equal to or less than the friction force. Considering there are no slippages on any contact area of thread, the following condition should be satisfied[11-12]

$$\sqrt{S_\tau^2 + S_b^2} \le \mu S_n \tag{14}$$

In order to determine the critical transverse load $[F_T]_C$, the relationship of S and S_T with the bolt preload F_p, additional bending moment M and the transverse loads F_f should be derived firstly.

3.2. Determination of S

As shown in Fig. 5, the resultant forces S can be broken up into force S_1 caused by the bolt preload F_p, and force S_2 caused by the additional bending moment *M*.

3.2.1. Determination of S_1 *Caused by Bolt Preload* F_P

In order to get the thread force S_1 at unit length generated by the bolt preload F_p, the global Cartesian coordinate system with ordinate origin *O* located at the intersection point of bolt axis and bearing surface of nut is established (see Fig.5). As shown in Fig. 7, the axial forces $F(z)$ and additional bending moment $M(z)$ at arbitrarily cross section of bolt will vary with the height based on the elastic deformation assumption of thread.

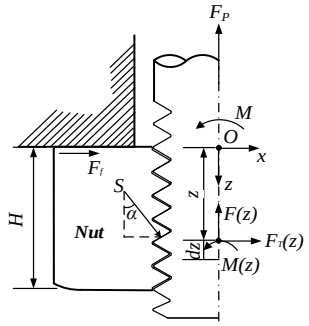

Fig. 7 Bolt force diagram

The axial strain of bolt shank ε_{1b} and the axial strain of nut ε_{1n} can be expressed as following

$$\begin{cases} \varepsilon_{1b} = \dfrac{F(z)}{A_b \cdot E_b} \\ \varepsilon_{1n} = \dfrac{F(z)}{A_n \cdot E_n} \end{cases} \tag{15}$$

where, A_b, A_n and E_b, E_n are the effective area and Young modulus of bolt shank and nut respectively.

Therefore, the forces $\mathrm{d}F(z)$ on $\mathrm{d}z$ is

$$\mathrm{d}F(z) = -S_1 \cos\alpha \cdot \mathrm{d}s \tag{16}$$

Where $\mathrm{d}s$ is the infinitesimal length of thread along the direction of the helix, and

$$\mathrm{d}s = \frac{\mathrm{d}z}{\sin\beta} \tag{17}$$

Substituting equation (17) into the equation (16), the following can be get

$$\mathrm{d}F(z) = \frac{-S_1 \cos\alpha \cdot \mathrm{d}z}{\sin\beta} \tag{18}$$

Therefore,

$$S_1 \cos\alpha = -\frac{\mathrm{d}F(z)}{\mathrm{d}z} \cdot \sin\beta \tag{19}$$

The axial elastic deformation of the unit width of the ISO metric triangular thread under the unit force as shown in Fig. 8 is sum of the deformation δ_1 caused by the bending, the deformation δ_2 caused by the shearing force, the deformation δ_3 caused by the inclination of the root, the deformation δ_4 and δ_5 caused by the shear deformation of the root and the radial expansion and contraction of the thread. The axial elastic deflections of unit length thread of bolt and nut are[16]

$$\left.\begin{aligned} \delta_{1b} &= 0.034\left(\frac{1-\nu_b^2}{E_b}\right) \\ \delta_{2b} &= 1.08\left(\frac{1+\nu_b}{E_b}\right) \\ \delta_{3b} &= 0.229\left(\frac{1-\nu_b^2}{E_b}\right) \\ \delta_{4b} &= 1.18\left(\frac{1-\nu_b^2}{E_b}\right) \\ \delta_{5b} &= 0.167(1-\nu_b)\frac{1}{E_b}\frac{D}{p} \end{aligned}\right\} \qquad \left.\begin{aligned} \delta_{1n} &= 0.073\left(\frac{1-\nu_n^2}{E_n}\right) \\ \delta_{2n} &= 1.15\left(\frac{1+\nu_n}{E_n}\right) \\ \delta_{3n} &= 0.294\left(\frac{1-\nu_n^2}{E_n}\right) \\ \delta_{4n} &= 1.14\left(\frac{1-\nu_n^2}{E_n}\right) \\ \delta_{5n} &= 0.167\left(\frac{D_0^2+D^2}{D_0^2-D^2}\right)\frac{1}{E_n}\frac{D}{p} \end{aligned}\right\} \tag{20}$$

Where, the sub-indices b and n represent the bolt and the nut respectively, ν is Poisson ratio, p is pitch, and D is the pitch diameter of bolt shank. D_0 is the outer diameter of nut.

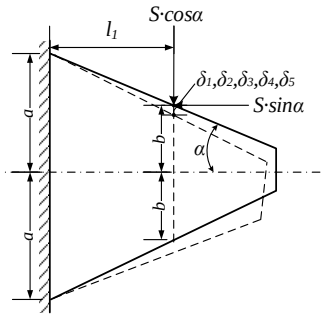

Fig. 8 The axial elastic deformation of thread

Therefore, the thread deformation of bolt shank and nut Δ_{1b} and Δ_{1n} are as following

$$\begin{cases} \Delta_{1b} = \delta_b \cdot S_1 \cdot \cos\alpha \\ \Delta_{1n} = \delta_n \cdot S_1 \cdot \cos\alpha \end{cases} \tag{21}$$

where,

$$\delta_b = \delta_{1b} + \delta_{2b} + \delta_{3b} + \delta_{4b} + \delta_{5b} = \frac{k_b}{E_b} \tag{22}$$

$$\delta_n = \delta_{1n} + \delta_{2n} + \delta_{3n} + \delta_{4n} + \delta_{5n} = \frac{k_n}{E_n} \tag{23}$$

in which, k_b, k_n are defined as the longitudinal elastic deformation coefficients of bolt thread and nut thread, which are related to the parameters of the bolt and nut and the Poisson's ratio as shown in equation (20). Therefore, the deformations δ_n and δ_b are linear to k_b and k_n in the elastic deformation of the thread.

However, the relationship between δ_n, δ_b and k_b, k_n can be effected by the surface roughness of the thread, thread coating etc. In order to describe the elastic deformation of the thread accurately, the deformation correction coefficient λ is introduced to correct the deformation of the thread. Therefore, the axial elastic deformation of the bolt and nut is corrected to

$$\delta_b = \frac{\lambda k_b}{E_b} \qquad \delta_n = \frac{\lambda k_n}{E_n} \tag{24}$$

Combined equation (19), (21) and (24), the following can be get

$$\begin{cases} \Delta_{1b} = -\dfrac{\lambda k_b}{E_b} \cdot \sin\beta \cdot \dfrac{\mathrm{d}F}{\mathrm{d}z} \\ \Delta_{1n} = -\dfrac{\lambda k_n}{E_n} \cdot \sin\beta \cdot \dfrac{\mathrm{d}F}{\mathrm{d}z} \end{cases} \tag{25}$$

In order to satisfy the deformation compatibility condition, the following equation should be satisfied

$$\varepsilon_{1b} + \varepsilon_{1n} = -\frac{\mathrm{d}\Delta_{1b}}{\mathrm{d}z} - \frac{\mathrm{d}\Delta_{1n}}{\mathrm{d}z} \tag{26}$$

Substituting equation (15) and (25) into (26) leads to

$$\frac{\mathrm{d}^2F}{\mathrm{d}z^2} = \omega^2 F \tag{27}$$

Where, $\omega = \sqrt{(\dfrac{1}{A_b E_b} + \dfrac{1}{A_n E_n}) / [(\dfrac{\lambda k_b}{E_b} + \dfrac{\lambda k_n}{E_n})\sin\beta]}$

The analytical solution of equation (27) is

$$F(z) = C_1 \sinh\omega z + C_2 \cosh\omega z \tag{28}$$

Considering the boundary conditions

$$\begin{cases} F(H) = 0 \\ F(0) = F_P \end{cases}$$

The equation (28) satisfies the above boundary condition, then the following can be easily got

$$F(z)=F_P\left(-\frac{\cosh\omega H}{\sinh\omega H}\sinh\omega z+\cosh\omega z\right) \tag{29}$$

Substituting equation (29) into (19) leads to

$$S_1(z)=\omega F_P\left(\frac{\cosh\omega H}{\sinh\omega H}\cosh\omega z-\sinh\omega z\right)\frac{\sin\beta}{\cos\alpha} \tag{30}$$

Equation (30) presents the expression of thread force S_1 at unit length generated by the bolt preload F_P.

3.2.2. Determination of S_2 Caused by Additional Bending Moment M

The thread forces S_2 at unit length generated by the additional bending moment M on the thread surface also varies with height, as shown in Fig. 7. The axial strain ε_{2b} of the bolt and the axial strain ε_{2n} of the nut are

$$\begin{cases}\varepsilon_{2b}=\dfrac{M(z)}{I_{by}\cdot E_b}\cdot\dfrac{d_2}{2}\cos\theta\\ \varepsilon_{2n}=\dfrac{M(z)}{I_{ny}\cdot E_n}\cdot\dfrac{d_2}{2}\cos\theta\end{cases} \tag{31}$$

in which, $M(z)$ is the additional bending moment of the bolt cross section at the *z* position. I_{by} and I_{ny} are the moment of inertia of the bolt and the nut about y-axis (see Fig. 5).

Similar to the solution method of $\mathrm{d}F(z)$ in the previous section, the additional bending moment $\mathrm{d}M(z)$ on $\mathrm{d}z$ is

$$\mathrm{d}M(z)=-\frac{S_2(z)\cos\alpha\cdot d_2\cos\theta\cdot\mathrm{d}z}{2\sin\beta} \tag{32}$$

Rearrange the equation, we get

$$S_2(z)\cos\alpha=-\frac{\mathrm{d}M(z)}{\mathrm{d}z}\cdot\frac{2\sin\beta}{d_2\cos\theta} \tag{33}$$

Similar to equation (21), the axial deformation of the bolt thread and the axial deformation of the nut thread are

$$\begin{cases}\Delta_{2b}=\delta_{1b}+\delta_{2b}+\delta_{3b}+\delta_{4b}+\delta_{5b}=\dfrac{\lambda k_b}{E_b}\cdot S_2(z)\cos\alpha\\ \Delta_{2n}=\delta_{1n}+\delta_{2n}+\delta_{3n}+\delta_{4n}+\delta_{5n}=\dfrac{\lambda k_n}{E_n}\cdot S_2(z)\cos\alpha\end{cases} \tag{34}$$

Substitute equation (33) into (34), the axial deformations Δ_{2b} and Δ_{2n} can be obtained as following

$$\begin{cases}\Delta_{2b}=-\dfrac{\lambda k_b}{E_b}\cdot\dfrac{\mathrm{d}M(z)}{\mathrm{d}z}\cdot\dfrac{2\sin\beta}{d_2\cos\theta}\\ \Delta_{2n}=-\dfrac{\lambda k_n}{E_n}\cdot\dfrac{\mathrm{d}M(z)}{\mathrm{d}z}\cdot\dfrac{2\sin\beta}{d_2\cos\theta}\end{cases} \tag{35}$$

In order to satisfy the deformation compatibility condition, the following equation should be satisfied

$$\varepsilon_{2b}+\varepsilon_{2n}=-\frac{\mathrm{d}\Delta_{2b}}{\mathrm{d}z}-\frac{\mathrm{d}\Delta_{2n}}{\mathrm{d}z} \tag{36}$$

If $E_b=E_n$, substitute equations (31) and (35) into the deformation coordination equation (36) to get

$$\frac{\mathrm{d}^2M(z)}{\mathrm{d}z^2}+\frac{2tg\theta}{d_2tg\beta}\cdot\frac{\mathrm{d}M(z)}{\mathrm{d}z}-\frac{1/I_{by}+1/I_{ny}}{\lambda k_b+\lambda k_n}\cdot\frac{d_2^2\cos^2\theta}{4\sin\beta}M(z)=0 \tag{37}$$

Equation (37) is a second-order linear differential equation with variable coefficients. The additional bending moment M can be obtained by solving the boundary value problem in the numerical solution. The boundary conditions are

$$\begin{cases}M(0)=M\\ M(H)=0\end{cases} \tag{38}$$

Therefore, by substituting $\mathrm{d}M/\mathrm{d}z$ obtained by equation (37) into equation (33), the force S_2 in the micro-region of unit length caused by additional bending moment M can be obtained.

3.3. Determination of S_T Caused by Transverse Load F_f

When the elastic deformation of the thread is considered, the transverse load also produces a shear stress that varies with position on the threaded surface, as shown in Fig. 7. The tangential strain γ_b of the bolt at the *z* position and the tangential strain γ_n of the nut are

$$\begin{cases}\gamma_b=\dfrac{f_bF_T(z)}{G_bA_b}\\ \gamma_n=\dfrac{f_nF_T(z)}{G_nA_n}\end{cases} \tag{39}$$

in which, G_b and G_n are the shear modulus of bolt and nut. $F_T(z)$ is the transverse load on the cross section of the bolt at the Z position. f_b and f_n are the shear shape coefficients of bolts and nuts,they equal to 0.9 and 2.0 respectively[17].

Similar to the solution method of $\mathrm{d}F(z)$ in the previous section, the tangential force $\mathrm{d}F_T(z)$ acting on $\mathrm{d}z$ is

$$\mathrm{d}F_T(z)=-\frac{S_T(z)\cdot\mathrm{d}z}{\sin\beta} \tag{40}$$

Rearrange the equation, we get

$$S_T(z)=-\frac{\mathrm{d}F_T(z)}{\mathrm{d}z}\sin\beta \tag{41}$$

According to the deformation formula of the thread under the radial force[16], the radial deformation u_b of the bolt thread and the radial deformation u_n of the nut thread can be calculated as following

$$\begin{cases}u_b=\dfrac{\xi k_b^r}{E_b}\cdot\dfrac{S_T(z)}{\cos\theta}\\ u_n=\dfrac{\xi k_n^r}{E_n}\cdot\dfrac{S_T(z)}{\cos\theta}\end{cases} \tag{42}$$

where, ξ is the radial deformation coefficient of the thread just as λ defined in equation (24).

In equation (42), k_b^r and k_n^r are the radial elastic deformation coefficients of bolt thread and nut thread, and their calculation formulas are

$$\begin{cases}k_b^r=(1-v_b)\dfrac{d_2}{2p}\\ k_n^r=(\dfrac{D_0^2+d_2^2}{D_0^2-d_2^2}+v_n)\dfrac{d_2}{2p}\end{cases} \tag{43}$$

The simultaneous equations (41) and (42), the radial deformations u_b and u_n of the bolt thread and the nut thread can be get respectively.

$$\begin{cases}u_b=-\dfrac{\xi k_b^r}{E_b}\cdot\dfrac{\mathrm{d}F_T}{\mathrm{d}z}\cdot\dfrac{\sin\beta}{\cos\theta}\\ u_n=-\dfrac{\xi k_n^r}{E_n}\cdot\dfrac{\mathrm{d}F_T}{\mathrm{d}z}\cdot\dfrac{\sin\beta}{\cos\theta}\end{cases} \tag{44}$$

In order to satisfy the deformation compatibility condition, γ_b, γ_n, u_b and u_n need to meet the following relationship

$$(\gamma_b+\gamma_n)\cos\theta=-\frac{\mathrm{d}u_b}{\mathrm{d}z}-\frac{\mathrm{d}u_n}{\mathrm{d}z} \tag{45}$$

In order to satisfy the deformation compatibility condition, the following equation should be satisfied

$$\frac{\mathrm{d}^2F_T(z)}{\mathrm{d}z^2}+\frac{2tg\theta}{d_2tg\beta}\cdot\frac{\mathrm{d}F_T(z)}{\mathrm{d}z}-\frac{2(1+\nu)\cos^2\theta}{(\xi k_b^r+\xi k_n^r)\sin\beta}\cdot\left(\frac{f_b}{A_b}+\frac{f_n}{A_n}\right)\cdot F_T(z)=0 \tag{46}$$

Equation (46) is a second-order linear differential equation with variable coefficients. The transverse load F_T can be obtained by solving the following boundary value problem in the numerical solution. The boundary conditions are

$$\begin{cases}F_T(0)=F_f\\F_T(H)=0\end{cases} \tag{47}$$

Therefore, by substituting $\mathrm{d}F_T/\mathrm{d}z$ obtained by equation (46) into equation (41), the transverse load S_T in the micro-region of unit length caused by the transverse load can be obtained.

4. Example analysis

The grade 6.8 standard hexagon bolt (GB/T 5783-2016, Hexagon head bolts—Full thread) is studied and the geometry parameters of bolt are listed in Tab. 1 according to the national standard hex head bolts of the People's Republic of China. The yield load of bolt shank is defined as F_y. Two load cases with the preload of $0.7F_y$ and $0.5F_y$ are presented in this paper, and the transverse load of 70% critical slippage load of bolt supporting surface(5.6kN and 4.0kN for two preload conditions) are applied on the bolted joint. The coefficient of friction between bolt, nut and gusset plate is set as 0.15.

Table 1
The geometry parameters of M16 bolt

Parameter	Value
Nominal diameter of thread（mm）	16
Bolt shank cross section moment of inertia（mm^4）	3216.99
Nut cross section moment of inertia（mm^4）	13069.02
Nut height（mm）	14
Clamping length（mm）	18
Pitch（mm）	2
Thread angle（°）	60

4.1. Analytical method

4.1.1. Distribution of bolt shank internal force

The internal forces are calculated with the above presented method. The axial force $F(z)$, the additional bending moment $M(z)$ and the transverse load $F_T(z)$ are obtained and shown in Fig. 9.

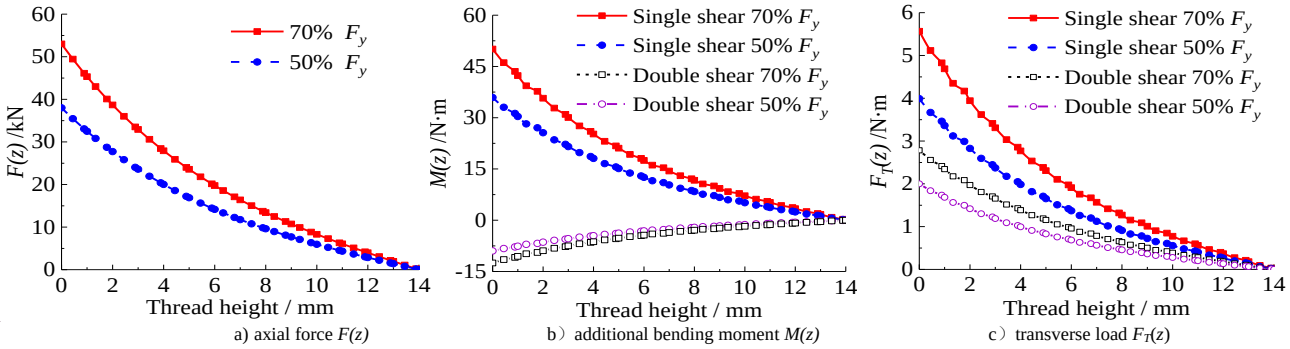

a) axial force $F(z)$　b）additional bending moment $M(z)$　c）transverse load $F_T(z)$

Fig. 9 Distribution of bolt shank internal forces

It can be seen in Fig. 9 that the axial load, additional bending moment and transverse load at the support surface of the nut (thread height equals to zero as shown in Fig. 7) are the largest. The internal forces are exponential increased as decrease of the thread height, which equal to zero when the thread height takes the maximum value. In the descend process of internal forces, the axial force decreases more smoothly, while the curves of the additional bending moment and the transverse load have slight fluctuations with the increasing of thread height which are due to the spiral change of thread. In addition, the additional bending moment in double shear planes bolted joint is a quarter of the single shear bolted joint, but the directions of the additional bending moment are opposite as shown in Fig. 9b. The transverse load of the bolt shank in the double shear planes bolted joint is half of the single shear as shown in Fig. 9c.

In order to study the changing of axial force, additional bending moment and transverse load of threads, the ratios of axial force, additional bending moment and transverse load of each thread to the applied load in the single and double shear planes bolted joint are used to description. Tab. 2 shows the variation of the ratio under the the preload of $0.7F_y$, and the variation range of the corresponding load ratio of the thread is in the parentheses. The thread number in Tab. 2 indicates that the thread is sequentially corresponding to the thread number from the initial engagement thread of the nut support surface until the last engagement thread. It can be seen that the axial force, additional bending moment and transverse load of the three threads near the nut support surface reach more than 50% of the applied load. However, the internal forces of the last three threads (thread number form 5 to 7) are less than 30% of the applied load. Therefore, the applied load is mainly acting on the first three threads(thread number form 1 to 3) near the nut support surface, and the loads on the other threads are relative small.

Table 2
Variation range of thread load

Thread number	Ratio of axial force to applied load	Ratio of additional bending moment to applied load	Ratio of transverse load to applied load
1	100%~73.0%（27.0%）	100%~71.3%（28.7%）	100%~100%（29.2%）
2	73.0%~52.7%（20.3%）	71.3%~50.4%（20.9%）	70.8%~49.8%（21.0%）
3	52.7%~37.2%（15.5%）	50.4%~34.9%（15.5%）	49.8%~34.3%（15.5%）
4	37.2%~25.2%（12.0%）	34.9%~23.3%（11.6%）	34.3%~22.8%（11.5%）
5	25.2%~15.6%（9.6%）	23.3%~14.3%（9.0%）	22.8%~13.9%（8.9%）
6	15.6%~7.4%（8.2%）	14.3%~6.8%（7.5%）	13.9%~6.6%（7.3%）
7	7.4%~0%（7.4%）	6.8%~0%（6.8%）	6.6%~0%（6.6%）

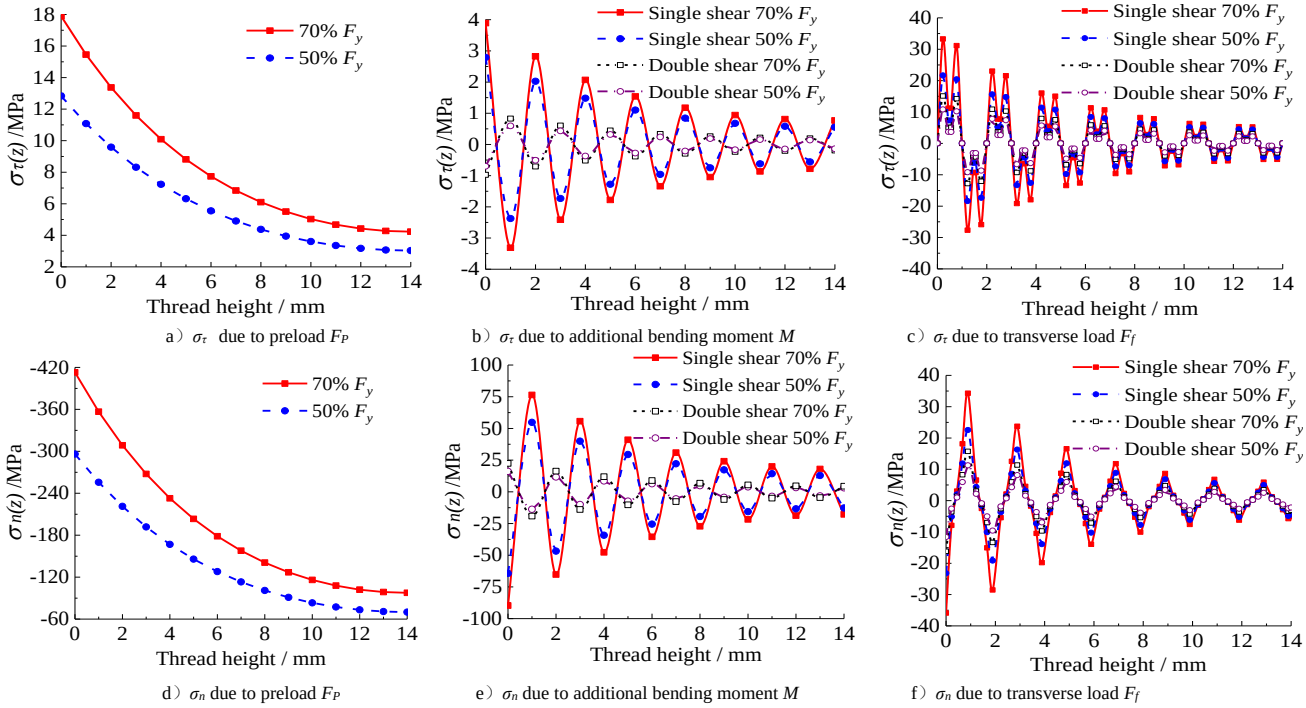

a）σ_τ due to preload F_P b）σ_τ due to additional bending moment M c）σ_τ due to transverse load F_f

d）σ_n due to preload F_P e）σ_n due to additional bending moment M f）σ_n due to transverse load F_f

Fig. 10 Stresses distribution on the thread surface

4.1.2. Thread stress

As presented above, the resultant forces S_1, S_2 and S_T can be determined by equation (30), (33), and (41) based on the calculation results of axial force $F(z)$, additional bending moment $M(z)$ and transverse load $F_T(z)$. Therefore, the tangential force S_τ, normal force S_n and radial force S_b applied on the thread at unit length can be calculated by equation (11)~(13). Since the theory assumes that the thread force is uniformly distributed in the radial direction, and S_1, S_2 and S_T are thread loads in the micro region of unit length, the tangential stress σ_τ, normal stress σ_n and radial stress σ_b can be got by the thread force S_τ, S_n and S_b, which are shown in Fig. 10 and Fig. 11.

Fig. 10a and Fig. 10d show the distribution of tangential and normal thread stress due to preload F_P. The thread stress at the support surface of the nut are both maximum and rapidly decrease as the distance from the nut support surface increases. The maximum tangential stress of the thread is 17.9MPa and 12.8MPa under the preload of $0.7F_y$ and $0.5F_y$, and the minimum tangential stress of the thread is 4.2MPa and 3.0MPa respectively. The maximum normal stress of the thread is 412.9MPa and 296.0MPa respectively, and the minimum normal stress is 97.6 MPa and 70.0 MPa respectively. It can be seen that the normal stress is much larger than tangential stress caused by preload F_p, and the stress increased with the increasing of preload.

Table 3
Tangential and normal stress of thread caused by additional bending moment

Thread number	Maximum tangential stress/MPa		Maximum normal stress/MPa	
	70%F_y	50% F_y	70% F_y	50% F_y
1	3.89(1.00)	2.79(1.00)	89.72(1.00)	64.33(1.00)
2	2.82(0.72)	2.02(0.72)	65.17(0.72)	46.72(0.72)
3	2.07(0.53)	1.48(0.53)	47.73(0.53)	34.22(0.53)
4	1.54(0.39)	1.10(0.39)	35.50(0.39)	25.45(0.39)
5	1.18(0.30)	0.84(0.30)	27.14(0.30)	19.46(0.30)
6	0.94(0.24)	0.68(0.24)	21.75(0.24)	15.59(0.24)
7	0.81(0.21)	0.58(0.21)	18.73(0.21)	13.43(0.21)

Fig. 10b and Fig. 10e are the distribution of tangential and normal stress due to the additional bending moment. It can be seen that the thread stress exhibits the distribution of nearly cosine functions with periodic decay as the distance from the nut support surface increases. Since the directions of tangential and normal stress are opposite in the single shear plane and double shear planes, and the stress in the single shear plane are quadruple of double shear planes, the single shear plane is taken as an example for analysis. The maximum tangential and normal stress of each thread due to additional bending moment are shown in Tab. 3. The stress attenuation coefficient in the parentheses are used to describe the degree of attenuation of the maximum stress in each thread, and its value is the ratio of the maximum stress of the thread to the maximum stress of the first thread. The attenuation coefficient of maximum tangential stress and the normal stress generated by the additional bending moment on each thread are exactly the same under these two transverse load, and the maximum tangential and normal stress of the last thread are 21% of the first thread. It can be seen that the tangential and normal stress of the thread generated by the additional bending moment near the nut support surface are greater than away from the nut support surface, and the attenuation law of the tangential and the normal stress of the thread is same and independent to the transverse load.

Table 4
Maximum tangential, normal and radial stress generated by transverse load F_f

	70% F_y	50% F_y	Ratio
Maximum tangential stress/MPa	63.90	45.81	1.4
Maximum normal stress/MPa	27.96	20.04	1.4
Maximum radial stress/MPa	7.26	5.21	1.4

Note: The negative values in the Figure represent the opposite direction, so the absolute value in the table is taken as the maximum stress.

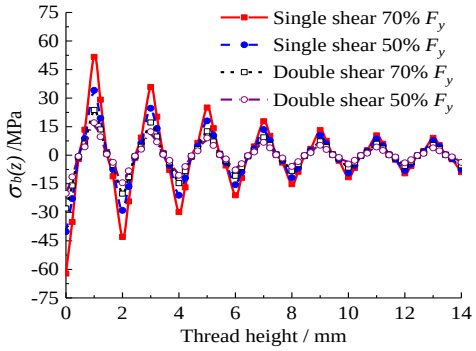

Fig. 11 Radial stress generated by transverse load F_f

As indicated in equation (12), the radial force S_b is only related to the transverse load S_T. The distribution of radial stress σ_b generated by the transverse load is shown in Fig. 11. It can be seen from Fig. 10c, Fig. 10f and Fig. 11 that the stress at the nut support surface are greatest and periodic decay as the distance from the nut support surface increases. Since the directions of normal, tangential and radial stress are identical in the single shear and the double shear planes, and the stress in the single shear planes are twice that of

the double shear planes, the single shear planes is also taken as an example for analysis. The maximum tangential, normal and radial stress of the two transverse loads and the ratio of maximum thread stress are summarized in Tab. 4. It can be seen that the ratio of tangential, normal and radial maximum stress under two transverse loads are all 1.4, so the tangential, normal and radial maximum stress of the threads are only related to the transverse loads.

Fig. 12 shows the thread stress at bolt preload of $0.7F_y$(53kN) and 70% critical slippage load of bolt supporting surface(5.6kN). We can see the thread stress in the three directions has a large stress near the nut support surface, and exhibit a periodic attenuation distribution as the distance from the nut support surface increases, whether it has single shear plane or double shear planes. The maximum values of tangential stress in the single shear plane and double shear planes appear in the position of $\theta = \pi/2 + 2k\pi$ (k is a positive integer of 0~6). Meanwhile, the maximum value of the tangential stress of the single shear plane relative to the double shear planes is reduced from 1.63 times to 1.56 times in each circle of thread. The absolute maximum of the normal stress appears at $\theta = 2k\pi$, and the maximum value of the single shear plane relative to the double shear planes is reduced from 1.32 times to 1.26 times. The maximum value of the radial stress appears at $\theta = 2k\pi$ or $\theta = \pi + 2k\pi$, and the maximum value of the single shear plane is twice that of the double shear planes. It can be seen that the thread force of the single shear plane is greater than that of the double shear planes, and the thread bearing capacity is mainly concentrated on the three threads near the nut support surface.

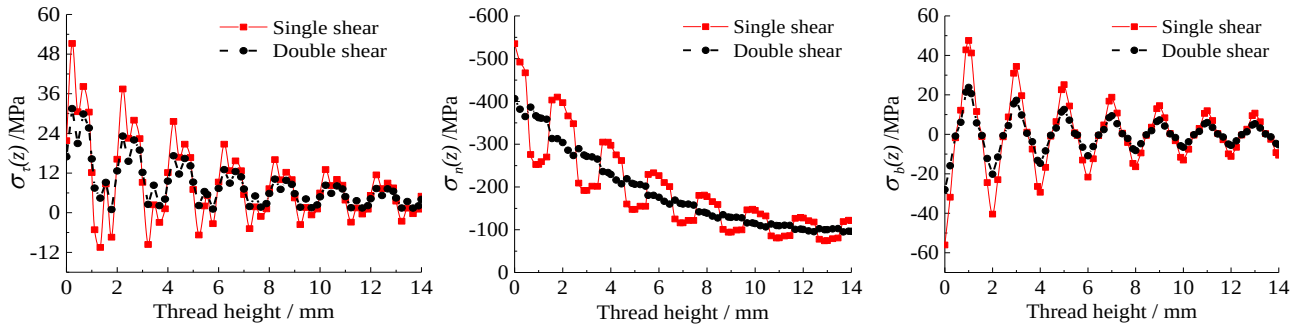

a）Distribution of σ_τ b）Distribution of σ_n c）Distribution of σ_b

Fig. 12 Thread stress under the combination of bolt preload and transverse load

4.2. Finite element analysis

In order to validate the presented theoretical method, the M16 standard hex bolt joint with single shear plane and double shear planes are analyzed with finite element method. During analysis 0.7Fy (53kN) bolt preload and 70% critical slippage load of bolt supporting surface(5.6kN) are selected as analytical conditions. The connecting plate used for the bolted joint has a modulus of elasticity of 206GPa, a Poisson's ratio of 0.3,and a density of 7850kg/m3. In the finite element models, three-dimensional tetrahedral elements are adopted in the bolts and nuts, and three-dimensional hexahedral elements are selected in the connecting plate. The mechanical properties of actual materials are simulated with multi-linear model. In order to correspond with the theoretical model, the connecting plates are assumed to be frictionless contact, and the other contact are set to frictional contact. In the single shear plane model, the boundary condition is that the right end of the bolted plate is fixed, and the left end is subjected to lateral load listed in Tab. 5. In the double-shear planes model, the right end of the upper and bottom plate are fixed, and the left end of the middle plate is subjected to lateral load.

As shown in Tab. 5, the nut is divided into two part along the plane formed by the axis and the line of transverse load. The solid line in Tab. 5 of the nut represents the stress distribution on the thread in the current part of the nut. In order to verify the attenuation law of thread stress in theoretical analysis, the attenuation coefficient of mean contact stress on each thread are listed in Tab. 6. As We can see in the table that the attenuation coefficients of the mean contact stress of the threads in single shear and double shear are the same, which is the same attenuation law as theoretical method. At the same time, the attenuation coefficient of mean contact stress on each thread obtained by the theory and simulation results is equal at the thread away from the nut support surface. The difference is small near the nut support surface, and the difference is greatest at the third thread.

Table 5
Finite element model and thread stress

	Finite element model	Stress distribution on the thread under combined load
Single shear	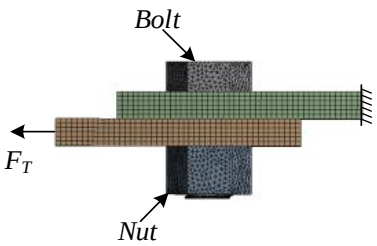	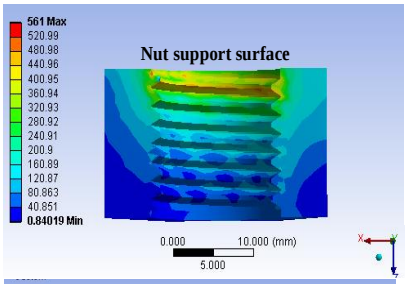
Double shear	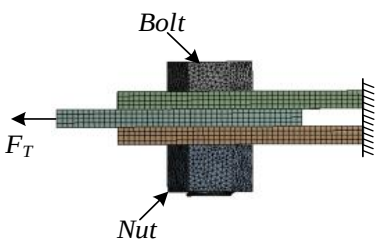	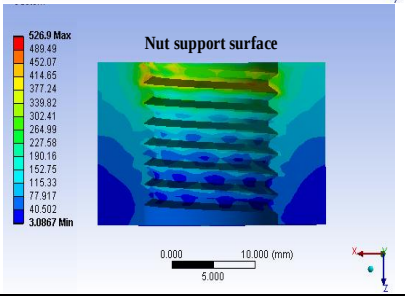

Table 6
Attenuation coefficient of mean contact stress on each thread

Thread number	Double shear model		Single shear model	
	Theoretical method	FEM	Theoretical method	FEM
1	1.00	1.00	1.00	1.00
2	0.72	0.70	0.72	0.68
3	0.53	0.49	0.53	0.48
4	0.39	0.37	0.39	0.36
5	0.30	0.29	0.30	0.28
6	0.24	0.24	0.24	0.24
7	0.21	0.19	0.21	0.19

4.3. Comparison and discussion

For the theoretical method, the axial deformation correction coefficient λ and the radial deformation correction coefficient ξ are both equal to 1.0 in equation (24), (34) and (42), and the mean contact stress on each contacted thread calculated from the theoretical method and that obtained by FEM are compared in Fig. 13. As can be seen in Fig.13 that the theoretical solution is close to the result of finite element simulation in single shear plane or double shear planes. With increasing of the distance from the nut support surface, the thread stress decreases gradually. The thread stress in single shear plane bolted joint is greater than that in double shear planes bolted joint, and the thread stress of the three threads near the nut support surface in single shear plane bolted joint is significantly larger than that in the double shear planes, which is consistent in the theoretical analysis. However, according to Fig. 13 and Tab. 6, the maximum error occurs at the third thread whether it is single shear plane or double shear planes bolted joint. In the third thread, the theoretical and analytical results of single shear plane bolted joint are 238MPa and 202MPa, and the relative error is 18%. The theoretical and simulation results of double shear planes are 256MPa and 211MPa, and the relative error is 21%.

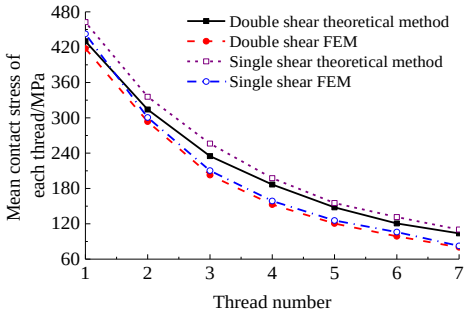

Fig. 13 Mean contact stress of each thread

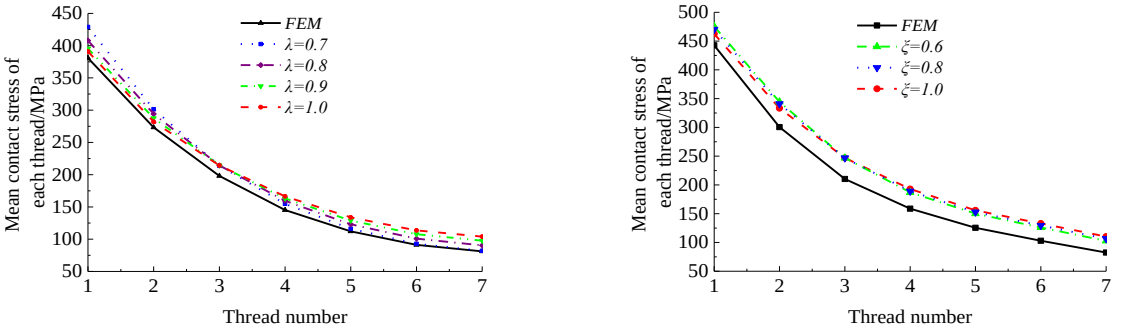

a) Comparison of axial deformation correction coefficient under preload b) Comparison of radial deformation correction coefficient under combined load

Fig. 14 Comparison of deformation correction coefficient

Table 7
Ratio of theoretical and simulation results on each thread under bolt preload and combined load

Thread number	Theoretical results/FEM results under bolt preload				Theoretical results/FEM results under combined load		
	λ=0.7	λ=0.8	λ=0.9	λ=1.0	ξ=0.6	ξ=0.8	ξ=1.0
1	1.13	1.07	1.04	1.03	1.07	1.06	1.05
2	1.10	1.08	1.05	1.03	1.15	1.13	1.11
3	1.08	1.08	1.08	1.08	1.17	1.17	1.17
4	1.07	1.10	1.12	1.15	1.18	1.19	1.21
5	1.04	1.10	1.15	1.19	1.20	1.22	1.24
6	1.02	1.11	1.18	1.25	1.22	1.26	1.29
7	1.01	1.11	1.20	1.28	1.25	1.29	1.34

In order to get more accurate stress on the thread surface, the correction coefficient of the axial deformation of the thread and the correction coefficient of the radial deformation proposed in the theory of this paper are discussed as a single shear model. Fig. 14a shows the effect of the axial deformation correction coefficient on the theoretical results under bolt preload with 0.7Fy (53kN). As can be seen in the figure that the mean contact stress near the third thread under different deformation coefficients is almost equal, and the thread stress calculated by theoretical method is slightly larger than the result of the finite element simulation. In order to facilitate the description of the mean contact stress of the thread considered axial deformation correction coefficient, the ratio of theoretical results and simulation results are listed in Tab. 7. It can be seen that when λ equal to 0.7, the ratio exhibits a tendency to decay as the distance from the nut support surface increases, and finally the ratio approaches to 1.0. Which means that the thread stress calculated by theoretical method can better describe the thread stress away from the nut support surface. When λ is equal to 0.8, 0.9 or 1.0, the ratio shows an increasing trend as the distance from the nut support surface increases, and the ratio approaches to 1.0 near the nut support surface. Which means that the thread stress calculated by theoretical method can better describe the thread stress near the nut support surface when λ is large. In addition, we can see that the ratios are equal in the third thread. Therefore, in the actual projects, different axial deformation correction coefficients can be determined as needed.

Fig. 14b shows the effect of the radial deformation coefficient on the theoretical results under combined load (a bolt preload of 0.7%F_y (53kN) and a 70% critical slippage load of bolt supporting surface(5.6kN)). According to the variation law of the axial deformation coefficient of the thread under the preload, λ equal to 0.8 are taken as the correction coefficient of the axial load in the combined deformation. Similar to the influence law of the axial deformation correction coefficient, the mean contact stress of the third thread is equal under different radial deformation correction coefficient, and the theoretical results are larger than the simulation results. Tab. 7 also listed the ratio to the finite element simulation results under different radial deformation correction coefficients. As can be seen in the table, the ratio is equal in the third thread which is same as the axial deformation coefficient. Meanwhile, the

corrected results are coincided with the FEM results much more better near the nut support surface. The difference is that the ratio increases with the increase of the distance from the nut under all the three radial deformation correction coefficients. Therefore, the stress of each thread can be obtained more accurately by reasonably selection of the axial deformation correction coefficient and the radial deformation correction coefficient.

5. Influence of bolt critical loosening load

It can be found that the bolted joint critical loosening load is related to many parameters in the theoretical method, such as bolt preload, friction coefficient of thread surface, bolt clamping length and shear plane number. In this paper the influence of these parameters on the critical loosening load are discussed, and the minimum critical loosening load in each thread are illustrated.

Fig. 15 shows the minimum critical loosening load for the thread under 30% (23kN), 50% (38kN), 70% (53kN) and 90% (68kN) bolt preload. It can be seen that the critical loosening load of the thread near the nut support surface is the smallest, and the minimum critical loosening load of the thread increases as the distance from the nut support surface increases. Therefore, the thread near the nut support surface is more prone to loosening under transverse load. The minimum critical loosening loads of the first thread are 1.82kN, 3.01kN, 4.19kN and 5.38kN respectively. The minimum critical loosening loads of the last thread are 2.24kN, 3.70kN, 5.15kN and 6.61kN respectively. It can be seen that as the preload increases, the minimum critical loosening load increases. However, the variation in the critical loosening load of the thread near the support surface is less than that away from the support surface.

Fig. 16 shows the minimum critical loosening load of the thread with different friction coefficient of the threaded surface, such as 0.25, 0.20, 0.15, 0.10. Similar to the influence of bolt preload, as increasing of the friction coefficient of the thread surface, the critical loosening load of the thread also increases. The minimum critical loosening loads of the first thread are 2.7kN, 4.19kN, 5.39kN and 6.39kN, and the minimum critical loosening loads of the last thread are 3.33kN, 5.15kN, 6.61kN and 7.83kN. It can be seen that as the friction coefficient of the thread surface increases, the critical loosening load of each thread also increases greatly, and the minimum critical loosening load of the thread away from the nut support surface is more affected.

Fig. 17 shows the minimum critical loosening load for each thread with bolt clamping lengths 6mm, 12mm, 18mm and 24mm. As can be seen in Fig. 17, the change in the bolted clamp length has almost the same effect on the minimum critical loosening load of each thread. At the same time, as the clamping length increases, the critical loosening load of the thread gradually decreases. The minimum critical loosening loads of the first thread are 4.70kN, 4.43kN, 4.19kN and 3.98kN, and the minimum critical loosening loads of the last thread are 5.81kN, 5.46kN, 5.15kN and 4.88kN. The ratio of the minimum critical loosening load is 1.18:1.12:1.05:1. Therefore, the magnitude of the change is less than the variation of the clamping length.

Fig. 18 shows the minimum critical loosening load for single shear plane and double shear plane bolted joint. As can be seen in the figure, the critical loosening load of the bolted joint will greatly increase with the increasing of shear plane number. The ratio of critical loosening load for double shear planes and the single shear plane in each thread is 2.178, 2.179, 2.180, 2.182, 2.183, 2.184 and 2.185. It can be seen that as the distance from the nut support surface increases, the critical loosening load of double shear plane has slight increased relative to the single shear plane, and the critical loosening load for double shear planes is approximately twice that of single shear plane.

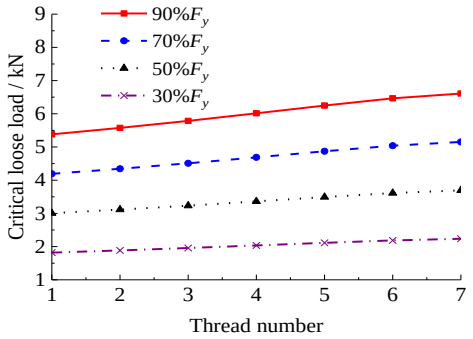

Fig. 15 Critical loosening load for different preload

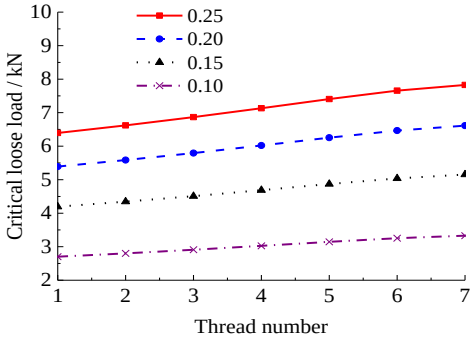

Fig. 16 Critical loosening load for different friction coefficients

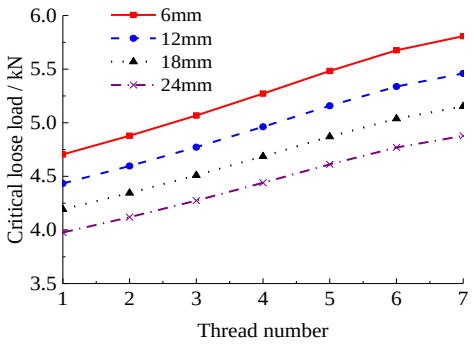

Fig. 17 Critical loosening load for different clamping lengths

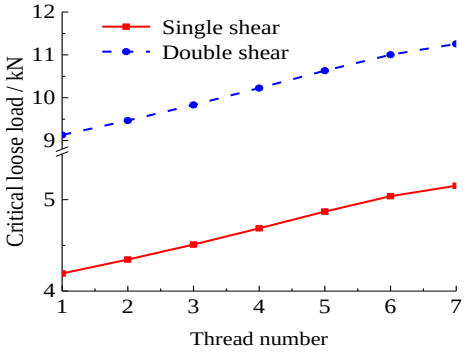

Fig. 18 Critical loosening load for single and double shear plane models

6. Discussions

In order to study bolt loosening, a new calculation method of critical loosening load for bolted joints is presented and modified by finite element analysis results in this paper. Theoretical research shows that the critical loosening load is determined by the transverse load on the bolted joint, which is caused by the axial force of member in transmission towers. However, the axial force of member can not be used to analyze the bolted joint self-loosening directly as the friction between the gusset plate is ignored in the theoretical model. Therefore the critical loosening loads calculated by the presented method are relative small compared with the real behavior of bolted joint, and the slippage load of bolted joint should be added in practical.

In the previous research, the distribution of bolt internal force and thread load are presented, and it shows that the thread load near the nut support surface is large, and the thread load away from the nut support surface is small. However, most researches use the finite element method to study the internal force and thread load, or establish a mathematical model based on the simulation results. Those method is essentially dependent on finite element simulation, and it also requires to establish a more accurate and reliable finite element model. Some researchers present the critical loosening load of bolted joints by experimental tests, and other researchers derived the theoretical calculation method based on the assumption of uniform distribution of thread load on all effectively engaged threads. However, the actual distribution of thread load is considered in the presented theoretical method, which led to more accurate critical loosening load of bolted joints.

The distribution of thread load, the load of bolt shank and the critical loosening load of bolted joints can be obtained by the given numerical calculation method in this paper. However, the bolted joints in transmission towers are often subjected to dynamic loads, which may cause some wear or contact surface condition changes, resulting in a large error with actual behavior.

Therefore, it is suggested to study the critical loosening load under the dynamic load, and carry out the experiment of loosening bolt. Then the theoretical method presented in this paper can be better corrected under the dynamic load.

7. Conclusions

The common transmission tower is a space structure formed by bolts and angle steel members. The reliability of bolt connection plays an important role in the safety and stability of the transmission tower. bolt connection Loosening can affect the safe and stable operation of the transmission tower. In this paper, a new theoretical method of critical loosening load of bolt joints is given, the distribution of thread stress is calculated, and the influence of structural parameters on the critical loosening load is analyzed. The conclusions are as following:

(1) A new theoretical method for the critical loosening load of bolted joint is presented, which is verified by finite element simulation, the modification of theoretical method are analyzed and correction coefficient are given.

(2) The maximum stresses of the threads in tangential, normal and radial directions are only related to the transverse loads and the maximum value of the radial stress for the single shear plane bolted joint in each thread is twice that of the double shear planes.

(3) The thread stress decreases rapidly as the distance from the nut support surface increases, and the thread stress of the first thread near the nut support surface is much greater than the stress of the last thread away from the nut support surface. The loads on the first three threads near the nut support surface take up more than 50% of the load on the entire bolt.

(4) The critical loosening load of the first thread near the nut support surface is the smallest. As the distance from the support surface increases, the critical loosening load of the thread increasing gradually.

(5) The increase of the bolt preload, friction coefficient of thread surface, and the shear plane number will increase the critical loosening load of the thread, which have a greater influence on the last thread away from the nut support surface. The increase of the bolt clamping length results in critical loosening load reduction, which has the same effects on the effective engagement threads.

Acknowledgement

The authors acknowledge the financial support provided by the Science and technology project of State Grid (No.SGHEBD00FCJS2000217).

Reference

[1] An, L. Q., Jiang, W. Q. and Liu, Y. P., et.al., "Experimental study of mechanical behaviour of angles in transmission towers under freezing temperature", Advanced Steel Construction, 2018, Vol. 14, No. 3, pp.461-478.

[2] Hussain, A., Liu, Y. P. and Chan, S. L., "Finite Element Modeling and Design of Single Angle Member Under Bi-axial Bending", Structures, 2018, Vol. 16, pp.373-389.

[3] Ibrahim, R. A. and Pettit, C. L., "Uncertainties and dynamic problems of bolted joints and other fasteners", Journal of Sound & Vibration, 2005, Vol. 279, No. 3, pp.857-936.

[4] Jiang, W. Q., Wang, Z. Q. and McClure, G., et.al., "Accurate modeling of joint effects in lattice transmission towers", Engineering Structures, 2011, Vol. 33, No. 5, pp.1817-1827.

[5] Može, P. and Beg, D., "Investigation of high strength steel connections with several bolts in double shear", Steel Construction, 2011, Vol. 67, No. 3, pp.333-347.

[6] Ungkurapinan, N., Chandrakeerthy, S. R. D. S. and Rajapakse, R. K. N. D., et.al., "Joint slip in steel electric transmission towers", Engineering Structures, 2003, Vol. 25, No. 6, pp. 779-787.

[7] Ahmed, K. I. E., Rajapakse, R. K. N. D. and Gadala, M.S., "Influence of bolted-joint slippage on the response of transmission towers subjected to frost-heave", Advances in Structural Engineering, 2009, Vol. 12, No. 1, pp. 1-17.

[8] Yang, F. L., Han, J. K. and Yang, J. B., et.al., "Analysis and experimental study on ultimate bearing capacity of structural members of cold-bending angle steel for transmission tower under axial compression", Power System Technology", 2010, Vol. 34, No.2, pp. 194-199.

[9] Orbison, J. G., McGuire, W. and Abel J. F., "Yield surface applications in nonlinear steel frame analysis", Computer Methods in Applied Mechanics and Engineering, 1982, Vol. 33, No.1-3, pp. 557-573.

[10] An, L. Q., Wu, J. and Jiang, W.Q., "Experimental and numerical study of the axial stiffness of bolted joints in steel lattice transmission tower legs", Engineering Structures, 2019, Vol.187, pp. 490-503.

[11] Jiang, W. Q., Liu, Y. P. and Chan, S. L., et.al., "Direct analysis of an ultrahigh-voltage lattice transmission tower considering joint effects", Journal of Structural Engineering, 2017, Vol. 143, No. 5, pp. 04017009.1-04017009.14.

[12] Pai, N. G. and Hessl, D. P., "Three-dimensional finite element analysis of threaded fastener loosening due to dynamic shear load", Engineering Failure Analysis, 2002, Vol. 9, No. 4, pp. 383-402.

[13] Dinger, G. and Friedrich, C., "Avoiding self-loosening failure of bolted joints with numerical assessment of local contact state", Engineering Failure Analysis, 2011, Vol. 18, No. 8, pp. 2188-2200.

[14] Izumi, S., Yokoyama, T. and Iwasaki, A., et.al., "Three-dimensional finite element analysis of tightening and loosening mechanism of threaded fastener", Engineering Failure Analysis, 2005, Vol. 12, No. 4, pp. 604-615.

[15] Pai, N. G. and Hess, D. P., "Experimental study of loosening of threaded fasteners due to dynamic shear loads", J Sound & Vibration, 2002, Vol. 253, No. 3, pp. 585-602.

[16] Zhang, M., Jiang , Y. Y. and Lee C. H., "Finite element modeling of self-loosening of bolted joints", Journal of Mechanical Design, 2007, Vol. 129, No.2, pp. 218-226.

[17] Yamatoto, A., "The theory and computation of threads connection",Yokendo, Tokyo, 1980, pp.39-54.

[18] Timoshenko, S. P. and Goodier, J. N., "Theory of Elasticity, third ed.", McGraw-Hill International Editions, 1970, pp.425-428.